Proc. of the Second Intl. Conf. on Advances In Mechanical and Robotics Engineering- AMRE 2014.

ISBN: 978-1-63248-031-6 doi: 10.15224/ 978-1-63248-031-6-142

Coupled Electromagnetic and Thermal-Fluid Analysis for a Permanent Magnet Synchronous Motor

Hao-Yen Chang and Yee-Pien Yang

***Abstract*—This paper proposes a coupling analysis of the electromagnetic and thermal-fluid fields in an interior permanent magnet motor for electric vehicles. Both electrical and magnetic materials have temperature-dependent properties. The power loss produced by the electromagnetic analysis reheats the motor and its rise in temperature alters the material properties as well as motor performance. The temperature-dependent power loss is used as a heat source to create a lumped-circuit thermal model in terms of equivalent thermal resistances and thermal capacitances, in order to investigate the transient response of the motor. Simulation results confirmed that coupled electromagnetic and thermal-fluid analysis is able to predict the performance of a motor prior to its prototyping.**

***Keywords*—electromagnetic analysis, thermal-fluid analysis, coupling simulation, temperature dependence.**

I. Introduction

The new global trend toward minimizing pollution has led to the rapid development of electric vehicles (EVs). One of the key components of their propulsion system used in EVs is the electric motor. Several motors are now commercially available, including permanent magnet motors, induction motors, and switched reluctance motors, but the permanent magnet (PM) motor is more suitable for passenger cars due to its compact size and high power and torque densities. However, the compact size of PM motors creates difficulties in heat dissipation. Consequently, electromagnetic and thermal-fluid analyses both become very significant in the design and analysis of EV motors.

The main electrical and magnetic materials of a PM motor include copper wire, silicon steel, and a magnet, which all have temperature-dependent properties. For example, the resistance of copper wire becomes larger as its temperature increases. The magnet can lose its magnetism when its temperature exceeds the Curie temperature. The resistance of silicon steel is also altered by temperature; thereby affecting the resulting eddy current and the corresponding power loss. The temperature-dependent power loss causes the motor to reheat and its rising temperature in turn causes additional changes in the material properties, further altering the electromagnetic performance of the motor.

Many researchers have proposed different modeling techniques to explain magnet demagnetization based on finite element (FE) analysis. Rosu et al. [1] used a classical Preisach hysteresis model to analyze the demagnetization state of PMs during fault conditions in a large synchronous motor. Fu and Ho [2] applied a linear model of normal BH curve to analyze the demagnetization behavior of PM motors. Ruoto et al. [3] introduced a thermal model that accounted for the temperature dependence of demagnetization behavior. Zhou et al. [4] presented a linear model that handled the complete demagnetization curve and temperature dependence of demagnetization behaviors. They proposed an iterative searching algorithm to identify a new worst working point along the gradient direction and to update the recoil during the entire transient solution process if a working point was below the knee point of the current recoil line. Fan et al. [5] discussed the thermal behavior of a PM motor on an EV during a real driving duty cycle. An improved core loss model was implemented by electromagnetic FE analysis, and the thermal behavior of the driving motor was analyzed by means of a lumped-circuit thermal model to predict the transient temperature distribution. Li et al. [6] presented a fast and precise electromagnetic-thermal model of a flux-switching PM motor. The power losses obtained by a 2D electromagnetic FE model were used as heat sources to calculate the temperature distribution by a lumped-circuit and FE thermal model.

Although many authors have included the temperature-dependent properties of the electrical and magnetic materials of a motor, few of them ever provided an efficient method for two-way coupled electromagnetic and thermal-fluid analysis of transient motor performance. In fact, the material property of the motor changes as the temperature varies, and then the motor performance changes to produce the observed temperature-dependent power losses. At low motor speeds, copper losses predominate, whereas marked core losses occur at high motor speeds. This paper proposes a combined analysis of both electromagnetics and thermal-fluid dynamics for a 50-kW interior PM (IPM) motor of an EV. Section II addresses motor specifications and the electromagnetic motor losses and their temperature dependence. Section III presents the coupled electromagnetic and thermal-fluid analysis, and Section IV draws conclusions.

II. Motor Specifications and Electromagnetic Loss

The 50-kW traction motor is a three-phase IPM motor with 42 slots and 8 magnet poles. The back electromotive force (back EMF) of the motor is close to a trapezoidal wave, and the motor is classified as a brushless dc motor. This motor drives an EV indirectly through a transmission with a gear reduction ratio of 6. Table I illustrates the specifications of the EV and the IPM motor.

In the energy conversion process, power losses of an electric machine can be categorized as copper loss, magnet loss, iron loss, and mechanical loss. The relationship between input power and output power is given by:

$$P_i = P_o + P_c + P_m + P_r + P_f \tag{1}$$

where P_i is the input electric power and $P_o = T\omega$ is the apparent output power in terms of the shaft torque T and the angular

Proc. of the Second Intl. Conf. on Advances In Mechanical and Robotics Engineering- AMRE 2014.

ISBN: 978-1-63248-031-6 doi: 10.15224/ 978-1-63248-031-6-142

velocity ω. Other terms represent motor losses: P_c is the copper loss, P_m is the magnet loss, P_r is the iron loss, and P_f is the mechanical loss. The motor efficiency is then expressed as:

$$\eta = \frac{T\omega}{T\omega + P_c + P_m + P_r + P_f} \times 100\% \cdot \quad (2)$$

TABLE I. SPECIFICATIONS OF MOTOR AND ELECTRIC VEHICLE

Electric Vehicle	
Weight	1800~2000 kg
Reduction ratio	6
Max. speed	>130 km/h
Climbing ability	>30%@30 km/h
Traction Motor	
Motor type	Three-phase IPM
Dimension	Φ 300 mm x 200 mm
Operating voltage	300 VDC
Current	Max. 350 A
Max. torque	200 Nm at 3000 rpm
Max. power	50 kW at 6000 rpm
Max. speed	40 kW at 8000 rpm
Cooling system	Water
Flow rate	11.2 L/min
Magnet	NdFeB
Temperature limit	Coil winding and magnet permissible operating temperature 100°C

A. *Temperature-Dependent Copper Loss*

Copper has an inherent property: its resistance increases as temperature rises. The linear approximation of the electrical resistance of copper is typically expressed as

$$R = R_{20}[1 + \alpha(T_c - 20)] \quad (3)$$

where R_{20} is the copper resistance at 20°C; α is the temperature coefficient of resistance at 20°C (which is 0.00404/°C); and T_c is the conductor temperature. For the 50-kW IPM motor, the phase resistance is 0.025 ohms at 20°C. The copper loss is proportional to the square of the input current and the resistance at a specific temperature. Fig. 1 shows that the copper loss in the IPM motor increases about 50% from 20°C to 160°C. This demonstrates that the copper loss in windings increases significantly as the temperature rises.

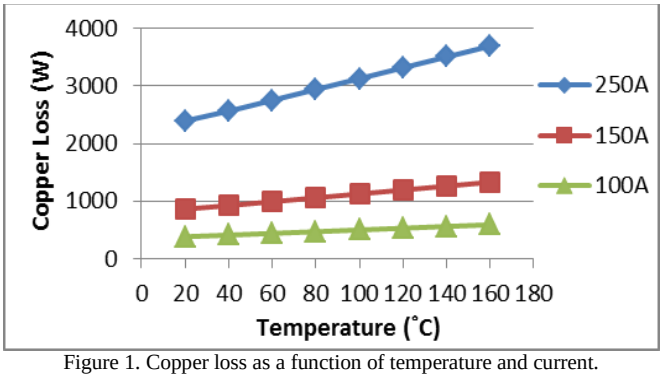

Figure 1. Copper loss as a function of temperature and current.

B. *Temperature-Dependent Magnet Loss*

The temperature-dependent remanence and coercivity of a magnet are usually expressed as:

$$B_r = B_{r20}\left[1 + \alpha_B\left(\theta_{PM} - 20^\circ\right)\right] \quad (4)$$

$$H_c = H_{c20}\left[1 + \alpha_H\left(\theta_{PM} - 20^\circ\right)\right] \quad (5)$$

where B_{r20} and H_{c20} are the remanence and coercivity, respectively, at 20°C; α_B (<0) and α_H (<0) are temperature coefficients for remanence and coercivity, respectively; and θ_{PM} is the temperature of the magnet. When the magnet temperature is higher than 20°C, the demagnetization curve is nonlinear. If the external excitation does not exceed the knee of the BH curve, the magnet will operate along its original recoil line and the magnet energy is reversible.

Eddy current loss is the main loss in PMs, especially during high-speed or high-frequency operations. The electromagnetic software, ANSYS Maxwell, is capable of determining the eddy current loss based on the temperature-dependent conductivity of the magnet and the flux density produced by the applied magnetomotive force (MMF). The higher-order time harmonics of the current waveform generated by the inverter are ignored in the following simulation due to the complexity of the waveform. Instead, only the fundamental of the current wave remains.

Fig. 2 illustrates the magnet loss for various phase currents and motor speeds at 20°C. Fig. 3 shows that the magnet loss drops as temperature rises. For example, when the phase current is 200 A, the magnet loss is 212.8 W at 20˚C, while it drops to 204.6 W at a higher temperature of 100°C.

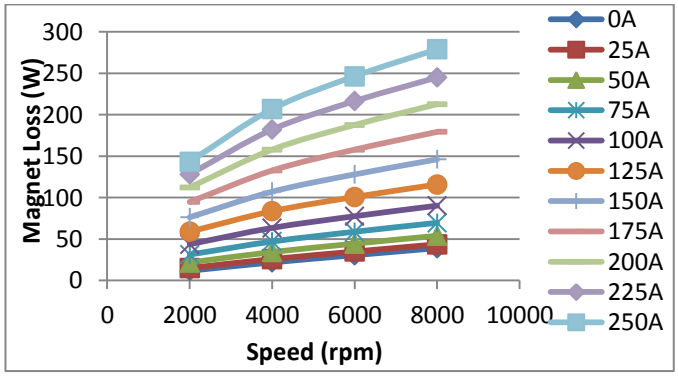

Figure 2. Magnet loss for various current inputs and motor speeds.

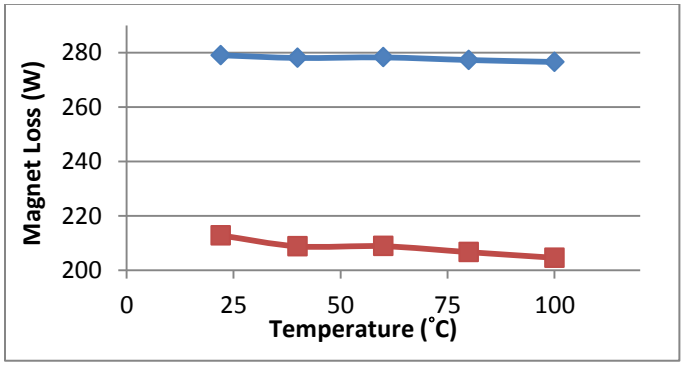

Figure 3. Magnet loss versus temperature for 250 A (diamonds) and 200 A (squares) at 8000 rpm.

Proc. of the Second Intl. Conf. on Advances In Mechanical and Robotics Engineering- AMRE 2014.

ISBN: 978-1-63248-031-6 doi: 10.15224/ 978-1-63248-031-6-142

C. *Temperature-Dependent Core Loss*

Core loss is composed of hysteresis loss and eddy current loss from the silicon steel in electric machines. Silicon steel is excited by the alternative or simply sinusoidal magnetic fields, and the core loss is approximately proportional to the square of the frequency of applied ac current. In other words, core loss affects motor performance more obviously in the high-speed region than in the low-speed region. The calculation of core loss is complicated. However, it is convenient for us to use the core loss data provided by the silicon steel manufacturer.

The manufacturer's data sheet usually provides core loss curves, which allow estimation of the material-dependent coefficients in the core loss polynomial as a function of flux density and frequency. Fig. 4 shows the simulation results where the core loss increases drastically as the motor speed increases. For the same motor speed, the core loss decreases as temperature rises. This is due to the demagnification effect of the magnet when the temperature rises.

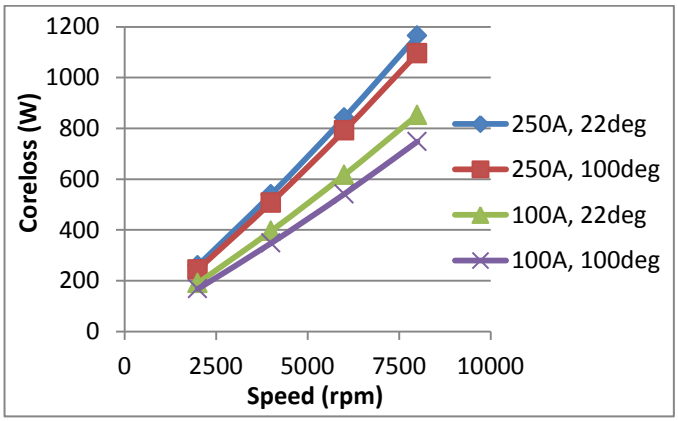

Figure 4. Core loss versus motor speed at different currents and temperatures.

III. Coupled Electromagnetic and Thermal-Fluid Analysis

Traditional one-way coupled electromagnetic and thermal-fluid analysis of a motor is performed when the electrical and magnetic material properties of the motor remain the same as they are at an initial temperature, e.g., 25°C. First, a constant electric power is supplied to the motor, and the power loss from the copper, magnet, and steel core is obtained using the ANSYS Maxwell software. Second, the power loss is imported to the thermal-fluid software, ANSYS Fluent, as the heat source; this heats the motor and causes the temperature to rise.

The proposed two-way coupled electromagnetic and thermal-fluid analysis takes into consideration the temperature dependence of the electrical and magnetic materials in the motor. First, we make a library of material properties for the copper, magnet, and steel as functions of temperature, flux density, and frequency. Second, in a specific temperature(e.g., 20~100°C), the power loss is calculated, using Maxwell, at each temperature (in increments of 10°C from 20°C) at a constant electric power supply in the steady state. Third, the power losses at different temperatures are imported to Fluent as heat sources to calculate the temperature response and its distribution from the initial motor temperature. During the iteration process, the power losses from the copper, magnet, and steel core vary as the temperature varies.

A. *Two-way Coupling Analysis*

Co-simulation can normally be accomplished using ANSYS Workbench. However, two-way automatic coupling analysis between Maxwell and Fluent for a transient response is not available in the current version, ANSYS 14.5. A manual operation for the two-way coupling analysis is realized according to Fig. 5.

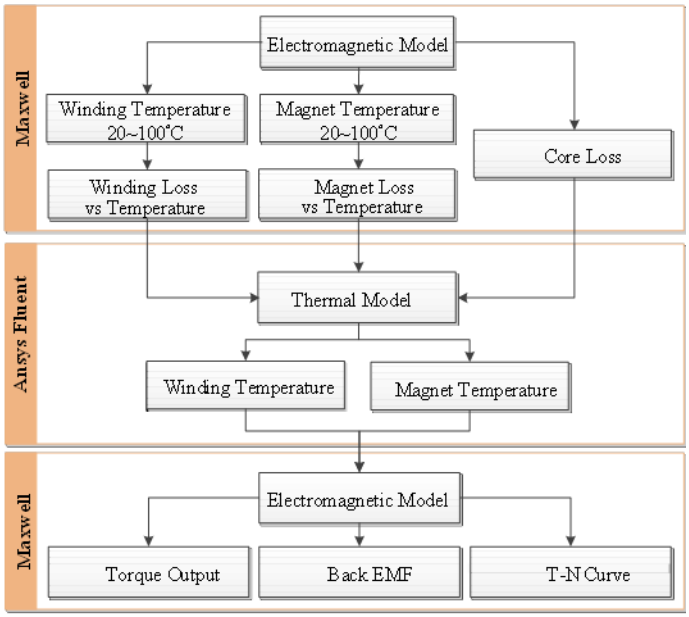

Figure 5. Flowchart of two-way electromagnetic and thermal-fluid co-simulation process.

Three main steps are designed for conducting a manual co-simulation process between the Maxwell electromagnetic analyzer and the Fluent thermal-fluid analyzer. The initial step involves the determination of various temperature-dependent losses in the stator winding, rotor magnet, and steel core. These loss data from Maxwell are imported to Fluent as temperature-dependent heat sources. The thermal-fluid simulation by Fluent provides the result of the temperature distribution of the motor. The final step is to import the average temperature determined in Fluent and to set the temperature of the motor components in Maxwell to investigate motor performances such as torque output, back EMF, and torque and speed curve at various temperatures.

Fig. 6 shows a cross-sectional view of the steady-state temperature distribution of the IPM motor under a constant electric power supply of 30 kW. The highest temperature of the motor occurs at the winding and the heat dissipates to stator core, rotor, and shaft, etc. The motor shell is coolest due to the forced heat convection from water channel and the natural heat convection of air on the surface of the motor shell. The inlet water temperature is 32.5°C, while the outlet temperature is 34.9°C at a flow rate of 11.2 L/min.

Proc. of the Second Intl. Conf. on Advances In Mechanical and Robotics Engineering- AMRE 2014.

ISBN: 978-1-63248-031-6 doi: 10.15224/ 978-1-63248-031-6-142

Taking the magnet as an example, the hottest spot occurs at the magnet center, as shown in Fig. 7. The average temperature of the magnet is 79°C in the one-way coupling analysis, while it is 85°C in the two-way coupling analysis. The temperatures of the other components of the motor are shown in Table II. The average temperature of each part of the motor is always higher when obtained by the two-way coupling analysis than by the one-way coupling analysis.

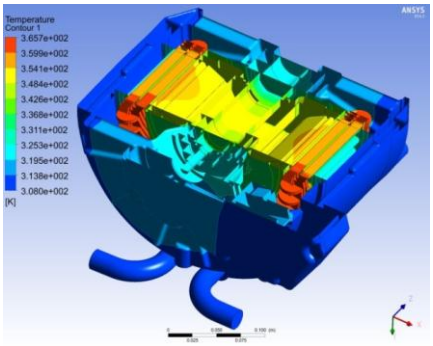

Figure 6. Steady-state temperature distribution of the IPM motor using a 30-kW electric power supply.

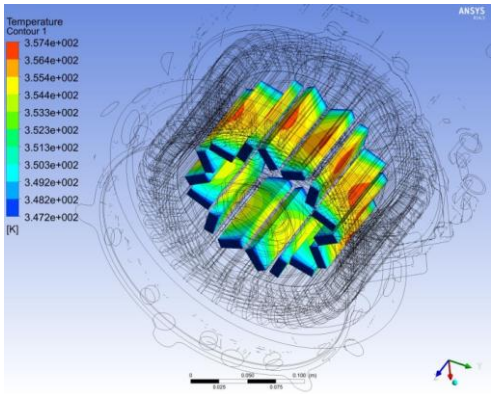

Figure 7. Steady-state temperature distribution at magnet under 30-kW electric power supply.

TABLE II. COMPARISON BETWEEN ONE-WAY AND TWO-WAY COUPLED ELECTROMAGNETIC AND THERMAL-FLUID ANALYSES

Component	CFD one-way	CFD two-way	Difference	
	Temp. (˚C)	Temp. (˚C)	˚C	%
Winding (hotspot)	93	103	10	9.7
Winding (average)	86	95	9	9.5
Shell	44	45	1	2.2
Stator	60	64	4	6.2
Magnet	79	85	6	7.1
Rotor	80	87	7	8
Shaft	71	76	5	6.6

B. *Motor Performance*

The thermal effect on motor performance is also investigated. When the motor was at the ambient temperature of 25°C, the induced back EMF was calculated as 56 V. From the two-way coupling analysis, when the motor was operated at 1500 rpm, the steady-state temperatures of the stator winding and magnet of the motor were 95°C and 85°C, respectively, and the induced back EMF dropped to 51.5 V. The corresponding back-EMF constant was 0.357 at 25°C, but it dropped to 0.328 when the stator winding and magnet temperatures were 95°C and 85°C, respectively. This infers that both the back-EMF value and the back-EMF constant decrease as temperature rises.

At the ambient temperature of 25°C, the average torque output was 154.32 Nm when the phase current was 300 A. The two-way coupling analysis revealed that when the steady-state temperatures of the stator winding and magnet of the motor were 95°C and 85°C, respectively, the average torque was reduced to 140.52 Nm at the phase current input of 300 A. Table III shows that the output torque is reduced by about 10-11% for the winding temperature rising from 25°C to 95°C. The corresponding torque and speed curves are also illustrated in Fig. 8. At the ambient temperature of 25°C, the maximum speed of motor reached 8900 rpm. The two-way coupling analysis indicated that a temperature of the winding and magnet of about 95°C and 85°C, respectively, led to an increase in the maximum speed to 9640 rpm. This indicates that when the operation temperature of the motor rises, the maximum torque decreases and the maximum speed increases.

TABLE III. TEMPERATURE EFFECT ON TORQUE OUTPUT

Phase Current (A)	Torque Output (Nm)		Difference (%)
	25°C	85/95°C	
25	13.77	12.27	11.00
50	27.33	24.40	10.83
75	40.68	36.34	10.74
100	53.91	48.16	10.73
125	66.98	59.89	10.66
150	79. 90	71.53	10.56
175	92.69	83.07	10.49
200	105.36	94.52	10.42
225	117.81	105.83	10.31
250	130.03	116.89	10.24

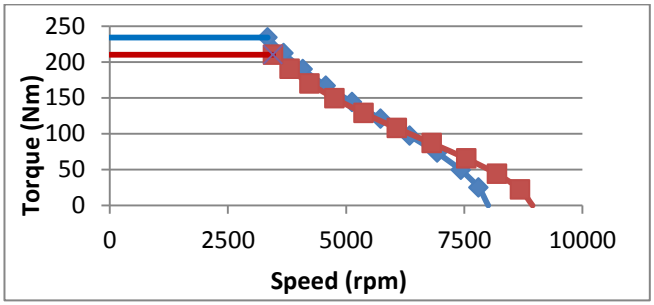

Figure 8. TN curves at winding temperatures of 25˚C (diamonds) and 95˚C (squares).

IV. Conclusions

This paper presents a new method of electromagnetic and thermal-fluid coupling analysis for a 50-kW IPM motor of an EV. Both one-way and two-way coupling analyses are introduced and compared. The two-way coupling analysis considers motor material properties to be functions of temperature. The temperature-dependent losses of the copper, magnet, and steel core are taken into consideration for analyzing the electromagnetic performance of the motor. These temperature-dependent properties are used to create a lumped-circuit thermal model in terms of equivalent thermal resistances, thermal capacitance, and power sources, in order to investigate the transient response of the motor. Simulation results show that the transient thermal response is close to the

Proc. of the Second Intl. Conf. on Advances In Mechanical and Robotics Engineering- AMRE 2014.

ISBN: 978-1-63248-031-6 doi: 10.15224/ 978-1-63248-031-6-142

result obtained from the two-way coupled electromagnetic and thermal-fluid analyses; the difference is within 10%. This confirms that the proposed two-way coupling analysis is able to predict the motor performance and represents an improvement over the traditional one-way coupling analysis.

Acknowledgment

This work was partially supported by the Ministry of Science and Technology of Taiwan under Contract MOST 102-2218-E-002-022, and the Industrial Technology Research Center, Hsinchu, Taiwan, ROC.

References

[1] M. Rosu, J. Saita, and A. Arkkio, "Hysteresis model for FE analysis of permanent-magnet demagnetization in a large synchronous motor under a fault," IEEE Trans.Magn., vol. 41, no. 6, pp. 2118–2123, 2005.

[2] W. N. Fu and S. L. Ho, "Dynamic demagnetization computation of permanent magnet motors using finite element method with normal magnetization curves," *IEEE Trans. Appl. Supercond*., vol. 20, no. 3, pp. 851–855, 2010.

[3] S. Ruoho, J. Kolehmainen, J. Ikaheimo, and A. Arkkio, "Interdependence of demagnetization, loading and temperature rise in a permanent- magnet synchronous motor," *IEEE Trans. Magn.*, vol. 46, no. 3, pp. 949–953, 2010.

[4] P. Zhou, D. Lin, and Y. Xiao, "Temperature-dependent demagnetization model of permanent magnets for finite element analysis," *IEEE Trans. Magn.*, vol. 48, no. 2, pp. 1031-1034, 2012.

[5] J. Fan, C. Zhang, and Z. Wang, "Thermal analysis of permanent magnet motor for the electric vehicle application considering driving duty cycle", *IEEE Trans. Magn.*, vol. 46, no. 6, pp. 2493-2496, 2010.

[6] G. Li, J. Ojeda, E. Hoang, M. Gabsi, and M. Lecrivain, "Thermal–electromagnetic analysis for driving cycles of embedded flux-switching permanent-magnet motors," *IEEE Trans. on Vehicular Technology*, vol. 61, no. 1, pp. 140-151, 2012.

About Author (s):

Hao-Yen Chang was born in Taiwan in 1984. He received a B.S. in mechanical engineering from University of Johannesburg in South Africa in 2008, and a M.S. in mechanical engineering from National Taiwan University in 2014. His research interests are on modeling optimal design and control of electric machines and drives for electromechanical actuation system.

Yee-Pien Yang received a B.S. and M.S. in mechanical engineering from National Cheng-Kung University in Taiwan, in 1979 and 1981, respectively, and a Ph.D. in Mechanical, Aerospace, and Nuclear Engineering from the University of California, Los Angeles in 1988. He is now a professor in the Department of Mechanical Engineering of National Taiwan University, leading the propulsion control laboratory and conducting research on the design and control of electro-mechanical systems, and assistive tool design for the disabled. He is also a researcher at the Industrial Technology Research (ITRI), Taiwan.